Hamburger Beiträge
zur Angewandten Mathematik

Model order reduction approaches for the optimal design of permanent magnets in electro-magnetic machines

A. Alla, M. Hinze, O. Lass, S. Ulbrich

Nr. 2014-23
October 2014

Model order reduction approaches for the optimal design of permanent magnets in electro-magnetic machines

A. Alla * **M. Hinze** * **O. Lass** ** **S. Ulbrich** **

* *Universität Hamburg, Bundesstr. 55, 20146, Hamburg, Germany (e-mail: {alessandro.alla, michael.hinze}@uni-hamburg.de).*
** *Technische Universität Darmstadt, Dolivostr. 15, 64293 Darmstadt, Germany (e-mail: {lass, ulbrich}@mathematik.tu-darmstadt.de)*

Abstract: In a electromagnetic machine with permanent magnets the excitation field is provided by a permanent magnet instead of a coil. The center of the generator, the rotor, contains the magnet. Our optimization goal consists in finding the minimum volume of the magnet which gives a desired electromotive force. This results in an optimization problem for a parametrized partial differential equation (PDE). We propose a goal-oriented model order reduction approach to provide a reduced order surrogate model for the parametrized PDE which then is utilized in the numerical optimization. Numerical tests will be provided in order to show the effectiveness of the proposed method.

Keywords: Proper Orthogonal Decomposition, Optimization, Model Order Reduction, Static Maxwell's equation

1. INTRODUCTION

Permanent magnet synchronous machines play an increasing role in applications demanding a highly dynamic behaviour of the drive and energy efficient speed and electromotive force control. To guarantee optimal operation of the drive, simplified analytical models are used in the control scheme of the machine. Designing a technical device is a complex process. For this purpose we model the machine by a magneto static Maxwell's equation. A first deep study on this model with an optimization problem is given in the PhD Thesis of Pahner (1998).

In this work we present an optimization problem related to the volume of the magnet. Due to the different configurations of the magnet we will introduce an affine decomposition which allows us to work on a fixed reference domain as proposed in Rozza et al. (2008).

The rather high computational expense of the optimization problem leads us to reduce the dimension of the problem by means of Proper Orthogonal Decomposition (POD). The POD method allows to reduce the degrees of freedom of the problem (see e.g., Gubisch et al. (2013)) and allows to design fast optimization methods which only need a few evaluations of the fully resolved objective function, and thus evaluations of the fully resolved PDE model, see e.g., APOD (Afanasiev et al. (2001)), TRPOD (Arian et al. (2002),Zahr et al. (2014)).

The outline of this paper is as follows. In Section 2 we give a brief introduction of our model problem. The optimization problem is described in Section 3. Section 4 is devoted to the model order reduction and its application to our optimization problem. Numerical results to demonstrate the effectiveness of the proposed methods are presented in Section 5. Finally a conclusion is drawn in Section 6.

⋆ This work is supported by the German BMBF in the context of the SIMUROM project (grant number 05M2013).

2. MODEL PROBLEM

Our mathematical model is build upon the Permanent Magnetic Synchronous Machines (PMSM) of Hennerberger et al. (1997). This PMSM is used as the base design, where some modifications have been added. The stator contains six slots per pole. A double-layer winding with two slots per pole per phase is used. Both, stator and rotor are made of laminated steel which is modeled by a relative permeability of $\mu_r = 500$ with vanishing conductivity. The length of the machine is 100 mm. Opposed to the original design, where five surface mounted magnets are used, we consider one buried permanent magnet in the rotor. This design provides greater mechanical strength for holding the magnet in place. The geometry is shown in Figure 1.

PMSMs are described by the magneto static approximation of Maxwell's equations. The model we consider in this work a parametrized elliptic partial differential equation (PDE) in terms of the magnetic vector potential (MVP) A,

$$\nabla \times (\mu \nabla \times A(\mu)) = J_{src}(\mu) - \nabla \times H_{pm}(\mu). \tag{1}$$

The boundary conditions are given by

$$A|_{BC} = A|_{DA} = 0, \quad A|_{AB} = -A|_{CD}, \tag{2}$$

where J_{src} is the source current density and H_{pm} is the coercivity of the permanent magnet, and the meaning of A, B, C, D is explained in Figure 1.

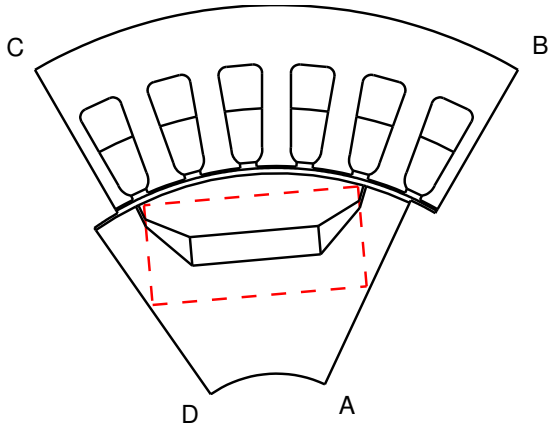

Fig. 1. Geometry for the model problem and the region for the affine decomposition marked with dashed lines.

In the planar 2D case, the finite element (FE) discretization leads to following parametrized linear system,

$$\mathbf{K}(\mu)\mathbf{u}(\mu) = \mathbf{j_{src}}(\mu) + \mathbf{j_{pm}}(\mu). \tag{3}$$

For the MVP we use the ansatz $A = \sum_{i=1}^{N} \mathbf{u}_i \varphi_i$, where φ_i are suitable ansatz functions. The FE system matrix $\mathbf{K}(\mu)$ emphasizes the dependency on the parameter μ. The parameter μ is related to the location and size of the permanent magnet. We consider a setting with a three dimensional parameter $\mu = (\mu_1, \mu_2, \mu_3)$. We use two parameters to describe the size of the permanent magnet, where μ_1 corresponds to its width and μ_2 to its height in mm. Additionally, since a PMSM with a buried permanent magnet is considered, we introduce the parameter μ_3 to describe the central perpendicular distance between the permanent magnet and the surface of the rotor in mm. To obtain a computationally fast model and to avoid remeshing when the parameter changes we require an affine decomposition. For this purpose we introduce a box around the permanent magnet (Figure 1, dashed line) in which we perform a domain decomposition, (see e.g. Rozza et al. (2008)) into L subdomains of triangular shape. As a consequence the system matrix can be written in the form

$$\mathbf{K}(\mu) = \mathbf{K}^{out} + \sum_{k=1}^{L} \theta^k(\mu)\mathbf{K}^k, \tag{4}$$

where $\mathbf{K}^{out}$ is the system matrix for the domain outside the box and $\mathbf{K}^k$, $k = 1, \ldots, L$, are the system matrices on the L domains inside the box obtained by the domain decomposition. The μ dependency of $\mathbf{K}$ is now only in the weight functions θ^k which are easy to evaluate. Note, that the same decomposition is made for the right hand side. This affine decomposition of the linear system is essential to obtain fast reduced order models, see Section 4. Furthermore, we only simulate one pole due to the symmetry of the problem.

3. OPTIMIZATION

Given the geometry presented in Figure 1, the goal of the optimization is to minimize the required material for the permanent magnet while maintaining the electromotive force E_0. In the mathematical model this leads to a cost function of the form

$$\min_{\mu \in M_{ad}} \bar{J}(\mu) := \mu_1\mu_2 + \rho \max(0, E^d - E_0(\mu, \mathbf{u}(\mu))), \tag{5}$$

where E^d is the desired electromotive force and

$$M_{ad} := \{\mu \in R^3 \,|\, \underline{\mu} \leq \mu \leq \overline{\mu}\}$$

with $\underline{\mu} = (1, 1, 5)$ and $\overline{\mu} = (\infty, \infty, 14)$ denotes the set of admissible parameters. The nonnegative parameter ρ is a penalization parameter and in our case set to 100. Note that for the computation of the electromotive force the solution to (3) is required, hence we have an optimization problem with a PDE constraint. Further, we only consider a 2D problem, hence we replace the volume by the area. In addition to the constraints defined in the admissible set we introduce the constraints

$$\mu_2 + \mu_3 \leq 15 \quad \text{and} \quad \mu_1 - \frac{2}{3}\mu_3 \leq \frac{50}{3}.$$

The first constraint is motivated by the affine decomposition. Since only a subdomain of the geometry is involved it is required that we stay within this region during the optimization process. The second constraint is a design constraint. It is required that the permanent magnet always has a certain distance to the rotor surface. Hence the depth of the magnet is linked to the width, which is expressed by this linear constraint.

The cost function (5) is not smooth due to the max operator. For the optimization we seek a smooth formulation of the minimization problem in order to apply derivative based methods. Therefore, we rewrite the problem by introducing a slack variable ξ. Setting $x = (\mu, \xi)$ we get the smooth optimization problem

$$\min_{x \in \mathbb{R}^4} J(x) := \mu_1\mu_2 + \rho\xi \tag{6}$$

subject to

$$G(x) := \begin{pmatrix} \mu_2 + \mu_3 - 15 \\ \mu_1 - \frac{2}{3}\mu_3 - \frac{50}{3} \\ E^d - E_0(\mu, \mathbf{u}(\mu)) - \xi \\ 1 - \mu_1 \\ 1 - \mu_2 \\ 5 - \mu_3 \\ -\xi \\ \mu_3 - 14 \end{pmatrix} \leq 0. \tag{7}$$

We now have an optimization problem that can be solved by standard methods presented in, e.g., Nocedal et al. (2006), Hinze et al. (2009) or Tröltzsch (2010). Let us give a brief outline of the methods utilized in the present work, including the computation of the derivatives. We apply here the approach using the sensitivity equations. Although computationally more expensive than the adjoint approach this method will be beneficial in the model

order reduction approach presented in Section 4. The sensitivities are required to compute the derivative of the electromotive force. Since E_0 is a linear operator we get

$$\frac{\partial E_0(\mu, \mathbf{u}(\mu))}{\partial \mu_i} = E_0(\mu, \mathbf{s}_i) \quad \text{for } i = 1, \dots, 3,$$

where $\mathbf{s}_i = \frac{\partial \mathbf{u}(\mu)}{\partial \mu_i}$ are the sensitivities. To obtain the sensitivities the linear sensitivity equations

$$\mathbf{K}(\mu)\mathbf{s_i}(\mu) = \mathbf{f}_i, \quad \text{for } i = 1, \dots, 3 \tag{8}$$

have to be solved with

$$\mathbf{f_i} = (\mathbf{j_{src}}(\mu) + \mathbf{j_{pm}}(\mu))_{\mu_\mathbf{i}} - \mathbf{K}_{\mu_\mathbf{i}}(\mu)\mathbf{u}(\mu).$$

Here the subindex μ_i indicate the derivative with respect to the i-th parameter. Note, that these derivatives are easy to compute due to the previousely introduced affine decomposition (4). The derivative of the matix $\mathbf{K}(\mu)$ is given by the derivatives of the functions $\theta^k(\mu)$.

To perform the numerical optimization we use the SQP method. This method provides fast convergence. To avoid the computationally expensive evaluation of the Hessian we use an approximation based on the damped BFGS update. To guarantee the convergence an Armijo backtracking strategy using a ℓ_1- penalty function is used (Nocedal et al. (2006)).

4. PROPER ORTHOGONAL DECOMPOSITION FOR PARAMETRIZED PROBLEMS

In this section, we explain the POD method for the approximate solution of the parametrized equation (3). To begin with, let us suppose to know the finite element solution $\mathbf{u}(\mu) \in \mathbb{R}^N$ for given parameter $\mu \in M_{ad}$. For this purpose let $\{\mu^j\}_{j=1}^n$ be a grid in M_{ad} and let $\mathbf{u}(\mu^j)$ denote the corresponding solutions to (3) for the grid points μ^j. We define the snapshots set $\mathcal{V} := \text{span}\{\mathbf{u}(\mu^1), \dots, \mathbf{u}(\mu^n)\}$ and determine a POD basis $\{\psi_1, \dots, \psi_\ell\}$ of rank ℓ by solving the following minimization problem:

$$\min_{\psi_1,\dots,\psi_\ell} \sum_{j=1}^{n} \alpha_j \left\| \mathbf{u}(\mu^j) - \sum_{i=1}^{\ell} \langle \mathbf{u}(\mu^j), \psi_i \rangle_W \psi_i \right\|_W^2$$
$$\text{s.t.} < \psi_j, \psi_i >_W = \delta_{ij} \quad \text{for } 1 \le i, j \le \ell, \tag{9}$$

where α_j are nonnegative weights, δ_{ij} denotes the Kronecker symbol, W is a positive definite $N \times N$ matrix and $\psi_i \in \mathbb{R}^n$. The weighted inner product used is defined as follows:

$$\langle \mathbf{u}, \mathbf{v} \rangle_W = \mathbf{u}^\top \mathbf{W} \mathbf{v}.$$

It is well-known (see Gubisch et al. (2013)) that problem (9) admits a unique solition $\{\psi_1, \dots, \psi_\ell\}$, where ψ_i denotes the $i-$th eigenvector of the selfadjoint linear mapping operator $\mathcal{R} : \mathbb{R}^n \to \mathbb{R}^n$, i.e. $\mathcal{R}\psi_i = \lambda_i \psi_i$ with $\lambda_i > 0$. where $\mathcal{R}$ is defined as follows:

$$\mathcal{R}\psi = \sum_{j=1}^{n} \alpha_j \langle \mathbf{u}(\mu^j), \psi \rangle_W \mathbf{u}(\mu^j) \quad \text{for } \psi \in \mathbb{R}^n.$$

Moreover

$$\sum_{j=1}^{n} \alpha_j \left\| \mathbf{u}(\mu^j) - \sum_{i=1}^{\ell} \langle \mathbf{u}(\mu^j), \psi_i \rangle_W \psi_i \right\|_W^2 = \sum_{i=\ell+1}^{d} \lambda_i.$$

4.1 POD approximation for state and sensitivities

We briefly recall how to generate the reduce order model by means of POD. Suppose we have computed the POD basis $\{\psi_i, \dots, \psi_\ell\}$ of rank ℓ. The weight matrix W is given by

$$\mathbf{W} = \mathbf{K}(\bar{\mu}) + \mathbf{M}(\bar{\mu}),$$

where $\bar{\mu}$ is a fixed reference parameter and $\mathbf{M}$ denotes the mass matrix. Then, we define the POD ansatz for the state $\mathbf{u}^\ell(\mu) := \sum_{i=1}^{\ell} \mathbf{w}_i^\ell \psi_i$. This ansatz in (3) leads to a $\ell-$dimensional system for the unknown $\{\mathbf{w}_i\}_{i=1}^{\ell}$, namely

$$\mathbf{K}^\ell(\mu)\mathbf{w}(\mu) = \mathbf{j}^\ell{}_{\mathbf{src}}(\mu) + \mathbf{j}^\ell{}_{\mathbf{pm}}(\mu). \tag{10}$$

Here the entries of the stiffness matrix $\mathbf{K}^\ell$ are given by $\langle \psi_i, \mathbf{K}(\mu)\psi_j \rangle_W$. The right hand side is composed of the projections $\langle \mathbf{j}_{src}(\mu), \psi_i \rangle_W$ and $\langle \mathbf{j}_{pm}(\mu), \psi_i \rangle_W$, respectively. Recall that due to the affine decomposition this projection has to be computed only once, and the system matrix can be written as

$$\mathbf{K}^\ell(\mu) = \mathbf{K}^{out,\ell} + \sum_{k=1}^{L} \theta^k(\mu) \mathbf{K}^{k,\ell},$$

where $\mathbf{K}^{out,\ell} = \langle \psi_i, \mathbf{K}^{out}(\mu)\psi_j \rangle_W$ and $\mathbf{K}^{k,\ell} = \langle \psi_i, \mathbf{K}^k(\mu)\psi_j \rangle_W$. The same structure can be used for the right hand side. Note that this is very important in order to obtain an efficient reduced order model since the system can be set up for different values of μ without the need of the original high dimensional matrices and right hand sides. In an analogous way we obtain the reduced sensitivity equation from (8). We need to make an ansatz for the sensitivities $\mathbf{s}_i$ and project the system onto the subspace spanned by the POD basis. Note that in the present work we use the same basis functions for the state $\mathbf{u}$ and the sensitivities $\mathbf{s}$. A better approximation property is achieved by adding the solution of the sensitivity equation to the snapshot set. More details are given in the next section.

4.2 The POD method for optimization problem

The selection of snapshots is crucial for the quality of the ROM. It is clear that the more information we provide about the system (i.e. the more snapshots details), the better and more accurate approximations we can achieve. Nevertheless, we want to avoid a too expensive offline stage. For this purpose we propose a goal-oriented approach for the computation of the POD basis functions. The goal is given by the difference between the electromotive force computed by the FE model and the reduced model, i.e., $|E_0(\mu, \mathbf{u}^\ell(\mu)) - E_0(\mu, \mathbf{u}(\mu))|$. The goal-oriented approximation approach aims at minimizing the error for a particular output function instead of minimizing the error in the state.

We start with a very coarse parameter space choosing only one parameter μ^0 and solve the full problem together with the sensitivity equations associated to this parameter. Then we compute the POD basis functions and perform the reduced optimization procedure. At the end of the process we find a new parameter μ^1 which is an approximation of the optimal desired design, we update the parameter set $\mathcal{D} = \{\mu^0, \mu^1\} \subset M_{ad}$, solve the full problem and the sensitivity equations related to the new parameter μ^1.

Then, we enlarge the snapshot set and compute new POD basis functions. We itereate this process until we reach the desidered convergence. The procedure is summarized in Algorithm 1.

Algorithm 1 (Goal-Oriented POD optimization)

Require: $\mu^0, \mathbf{u}(\mu^0), \mathcal{V} = [], k = 0, tol$

1: **while** $|E(\mu^k, \mathbf{u}^\ell(\mu^k) - E(\mu^k, \mathbf{u}(\mu^k))| > tol$ **do**
2: Compute sensitivity $\mathbf{s}_i(\mu^k)$, for $i = 1, 2, 3$.
3: Set Snapshots set
$$\mathcal{V} = [\mathcal{V}, \mathbf{u}(\mu^k), \mathbf{s}_1(\mu^k), \mathbf{s}_2(\mu^k), \mathbf{s}_3(\mu^k)]$$
4: Compute POD basis functions $\{\psi_i\}_{i=1}^{\ell}$ with $\ell = \text{rank}(\mathcal{V})$
5: Find μ^{k+1} solving the optimization problem utilizing the reduce order model
6: Compute $\mathbf{u}^\ell(\mu^{k+1})$ and $E(\mu^{k+1}, \mathbf{u}^\ell(\mu^{k+1}))$.
7: Compute $\mathbf{u}(\mu^{k+1})$ and $E(\mu^{k+1}, \mathbf{u}(\mu^{k+1}))$
8: Set k=k+1
9: **end while**

In our simulations this approach turns out to be the most efficient since it avoids long offline computations.

5. NUMERICAL EXPERIMENTS

This section presents numerical tests in order to show the performance of our proposed methods. All the numerical simulations reported in this paper are performed on an iMac with an Intel Core i5, 2.7 Ghz and 8GB RAM using MATLAB®. We will present three test cases. In the first experiment we show the performance of the reduced order model obtained by the POD method. The second and the third experiment focus on the optimization problem, where we first perform the optimization only using the FE method and compare the performance to the strategy proposed in Algorithm 1.

5.1 Test 1

The first test concerns the parametric model order reduction. We focus on two different snapshot sets: one is given by the PDE solutions corresponding to the corners of the parameter space, the second snapshot set is computed on an equidistant grid with grid size one. In the first case we have only eight snapshots, while in the second case we have 1170 snapshots. In Table 1 we show the maximum relative error in the POD approximation with the poor (second column, err_c) and with the rich (third column, err_f) snapshot span. As expected, the error in the third column is less than the error in the second column when varying the number of POD basis functions. Here the relevance of the snapshot set for the approximation quality can clearly be seen.

Figure 2 shows the behavior of the maximum relative error with respect to the number of POD basis functions. The Figure refers to the rich snapshot span (err_f). Moreover, we present the decay of the associated eigenvalues λ_i. From the decay of the eigenvalues it can be seen that we are able to reduce the dimension of the discrete state equation significantly.

Summarizing this experiment we can see that the POD method is able to gererate a reduced order model of good quality. Furthermore, the choice of the snapshots are essential since the reduced order model is only valid in a neighbourhood of the paramerter μ chosen to build the reduced order model. This is also observed in the optimization procedure using Algorithm 1.

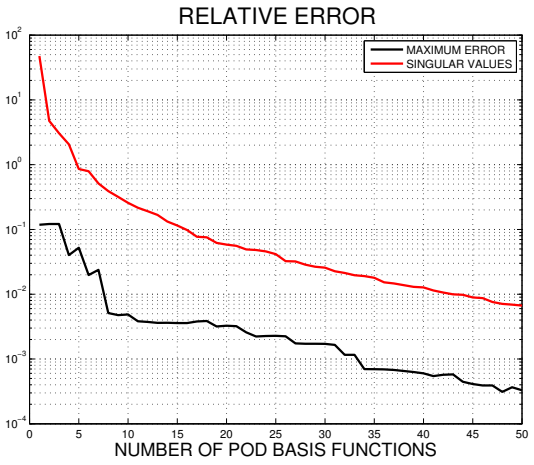

Fig. 2. Decay of the relative error and the eigenvalues.

5.2 Test 2

In this experiment we present the results for the optimization process using the FE model. The initial parameter choice is $\mu^0 = (19, 7, 7)$, and the desired electromotive force is set to $E^d = 30.3702$. Note that this particular choice corresponds to $E^d = E_0(\mu^0, \mathbf{u}(\mu^0))$. Further the volume ($V$) of the permanent magnet for the initial condition is $133mm^3$. The iteration history of the optimization routine is shown in Table 2. The optimal design is obtained with $\mu^{opt} = (21.071, 2.980, 6.607)$ and the corresponding volume is $62.798mm^3$. This corresponds to a reduction of more than 50% compared to the initial configuration. Moreover, Table 2 shows the norm of the gradient of the cost function in the third column. Once we are close to the optimal solution we can observe the fast quadratic convergence of the proposed method.

In Figure 3 we show the initial configuration. Comparing this to the optimal design shown in Figure 4 the significant reduction in the volume can be clearly seen.

Although the CPU time for our function evaluation is only 2.5s, this method is rather expensive since we needed 10 iterations to reach the optimal design. Each iteration needs the solution of 4 PDEs: one solution of (3) and three solves for the sensitivity equations (8). Summarizing, we have to solve 40 PDEs to achieve the optimal design. The dimension, in this example, is still rather moderate with

Table 1. Test 1: Comparison of maximum relative error of the reduced order model for different snapshot sets.

ℓ	err_c	err_f
3	0.0402	0.1002
4	0.0522	0.0657
5	0.0198	0.0577
6	0.0238	0.0592
7	0.0051	0.0584

Table 2. Test 2: Iteration history of the optimization algorithm using the FE model.

iter	J	$\|\nabla J\|$	μ
0	133.000	102.0294	(19.000 7.000 7.000)
1	105.248	5.752917	(19.136 5.500 6.500)
2	85.601	1.705679	(19.566 4.375 6.446)
3	75.466	2.031486	(20.106 3.753 6.732)
4	59.608	3.716464	(20.777 2.869 6.166)
5	62.196	1.497623	(21.163 2.939 6.746)
6	62.741	0.197684	(21.062 2.979 6.593)
7	62.796	0.010143	(21.071 2.980 6.607)
8	62.796	0.000123	(21.071 2.980 6.607)
9	62.796	0.000000	(21.071 2.980 6.607)

Solution u^0 ($E_0 = 30.3702$, $V = 133$)

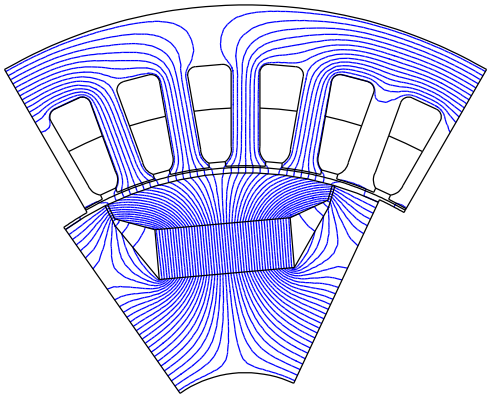

Fig. 3. Solution $\mathbf{u^0}$ to system (3) for the parameter μ^0.

only 8128 discretization points. We note that the number of unknowns and the related computational expenses dramatically increase if we simulate the whole machine or consider the 3D case.

5.3 Test 3

In the last experiment we combine the results from the previous two experiments and Algorithm 1. Table 4 shows that the snapshots set was updated once. Note that in every update we have to solve the system (3) and the sensitivity equations (8) in the full space. This is the most expensive part of the proposed algorithm. We solve only eight PDEs in this approach. Every iteration is the result of an optimization routine computed in the reduced space which is cheap since the $\ell-$dimensional problem is much smaller than the full problem. In fact each iteration in Table 3 considers the solution of four reduced equations. As we can see this algorithm needs to solve eight FE systems and 60 reduced systems. Compared to the computational costs of the optimization utilizing only the FE model we have a reduction in the computational cost of approximately a factor of five although the CPU time for the whole process is approximately 1s.

Solution u^{opt} ($E_0 = 30.3702$, $V = 62.7965$)

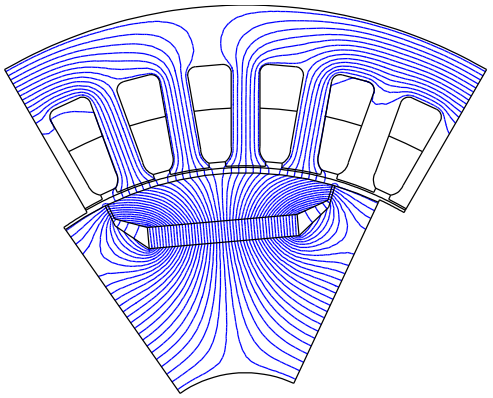

Fig. 4. Solution $\mathbf{u^{opt}}$ to system (3) for the parameter μ^{opt} obtaind by the optimization process.

The results obtained by the reduced approach are almost the same as the one obtained by the more expensive FE problem. In Table 4 the values for the electromotive force are compared when computed with the FE model and the reduced model. Here it can be seen that in the second iteration of Algorithm 1 the difference already is less than 10^{-4}, which is the chosen accuracy tolerance in this algorithm.

Table 3. Test 3: Opimization history utilizig Algorithm 1

iter	J	$\|\nabla J\|$	μ
0	133.000	102.0294	(19.000 7.000 7.000)
1	105.248	5.712287	(19.136 5.500 6.500)
2	85.706	1.767354	(19.590 4.375 6.482)
3	76.332	1.863950	(20.069 3.803 6.677)
4	59.643	3.352590	(20.751 2.874 6.126)
5	62.691	1.170096	(21.071 2.975 6.607)
6	63.053	0.133491	(21.007 3.001 6.511)
7	63.072	0.005441	(21.018 3.001 6.528)
8	63.072	0.000048	(21.018 3.001 6.527)
0	63.072	102.2290	21.018 3.001 6.527)
1	62.906	0.134651	(21.088 2.983 6.632)
2	62.795	0.074026	(21.069 2.980 6.604)
3	62.797	0.002143	(21.070 2.980 6.606)
4	62.797	0.000047	(21.070 2.980 6.606)

Table 4. Test 3: Comparison of the electromotive force computed from the $\mathbf{u}$ and $\mathbf{u}^\ell$ during the optimization process utilizing Algorithm 1.

iter	$E_0(\mu, \mathbf{u}(\mu))$	$E_0(\mu, \mathbf{u}^\ell(\mu))$	V
0	30.370231	30.370231	133.000000
1	30.393726	30.370231	63.072370
2	30.370245	30.370231	62.796700

6. CONCLUSION AND PROSPECTS

We present an algorithm for the optimal design of a permanent magnet in electro-magnetic machines. The algorithm allows to reduce the computational cost of the problem and at the same to provide an accurate approximation of the design as confirmed by the numerical tests.
Future work will include nonlinear problems and a possible extension to a 3D model, where we expect to observe an improved speed-up of the CPU time needed for optimization, and to deal with non-linear models.

REFERENCES

K. Afanasiev and M. Hinze. Adaptive control of a wake flow using proper orthogonal decomposition. *Lecture Notes in Pure and Applied Mathematics 216*, 317-332. Shape Optimization & Optimal Design, Marcel Dekker, 2001.

E. Arian, M. Fahl and E. Sachs. Trust-region proper orthogonal decomposition models by optimization methods. *In Proceedings of the 41st IEEE Conference on Decision and Control, Las Vegas, Nevada*, pages 3300 3305, 2002.

M. Gubisch and S. Volkwein. Proper Orthogonal Decomposition for Linear-Quadratic Optimal Control. *Submitted*, 2013.

M. Hinze, R. Pinnau, M. Ulbrich and S. Ulbrich. *Optimization with PDE Constraints. Mathematical Modelling: Theory and Applications, 23.* Springer Verlag, 2009.

S. Hennerberger, U. Pahner, K. Hameyer and R. Belmans. Computation of a highliy satured permanent magnet synchronous motor for a hybrid electric vehicle. *IEEE Trans. Magn.*, vol. 33, no. 5, pp. 4086-4088, 1997.

J. Nocedal and S.J. Wright. *Numerical Optimization, second edition.* Springer Series in Operation Research, 2006.

U. Pahner. A general design tool for the numerical optimization of electromagnetic energy transducers. *PhD Thesis*, KU Leuven, 1998.

G. Rozza, D.B.P. Huynh and A.T. Patera. Reduced Basis Approximation and a Posteriori Error Estimation for Affinely Parametrized Elliptic Coercive Partial Differential Equations. *Arch. Comput. Methods. Eng.*, vol.15. pages 229-275, 2008.

F. Tröltzsch. *Optimal Control of Partial Differential Equations: Theory, Methods and Application*, American Mathematical Society, 2010.

M. Zahr and C. Farhat. Progressive Construction of a Parametric Reduced-Order Model for PDE-Constrained Optimization. *International Journal for Numerical Methods in Engineering*, in press, 2014.